LEVEL II

AD A091993

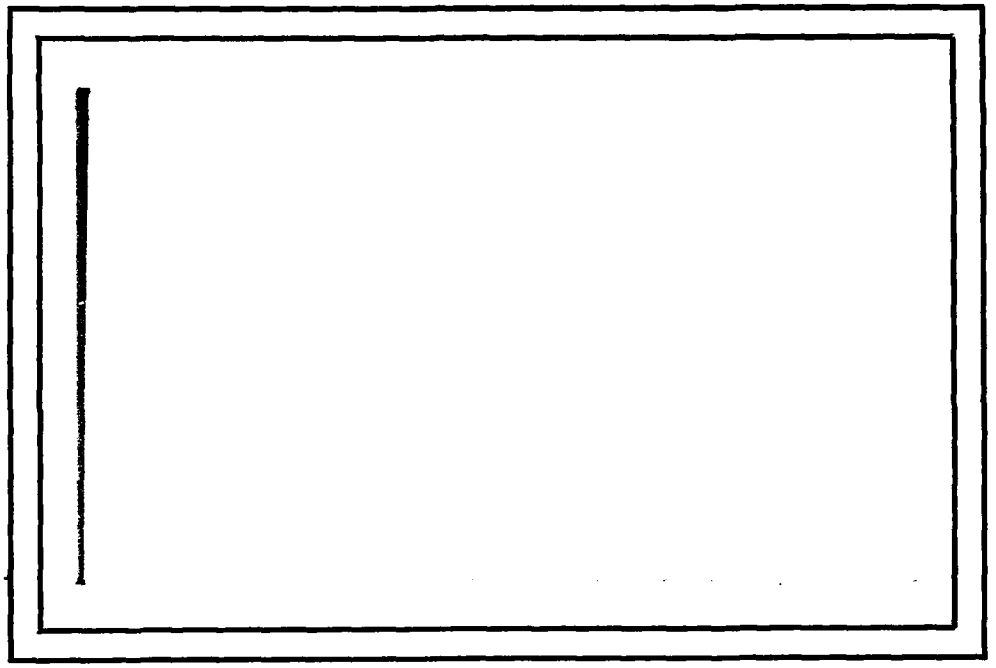

UNIVERSITY OF MARYLAND
COMPUTER SCIENCE CENTER

COLLEGE PARK, MARYLAND
20742

DISTRIBUTION STATEMENT A
Approved for public release;
Distribution Unlimited

DDC FILE COPY

DTIC
ELECTE
NOV 25 1980
S D
D

80 11 14 079

LEVEL II

(1)

TR-900
DAAG-53-76C-0138

May, 1980

IMAGE APPROXIMATION FROM GRAYSCALE "MEDIAL AXES"

See 1473 in Tech.

Shyuan Wang
Angela Y. Wu
Azriel Rosenfeld

Computer Vision Laboratory
Computer Science Center
University of Maryland
College Park, MD 20742

ABSTRACT

Several types of gray-weighted "medial axes" have been defined. This paper shows that one of them, the min-max medial axis, can be used to reconstruct good approximations to the original image based on a relatively small amount of information.

The support of the Defense Advanced Research Projects Agency and the U.S. Army Night Vision Laboratory under Contract DAAG-53-76C-0138 (DARPA Order 3206) is gratefully acknowledged, as is the help of Kathryn Riley in preparing this paper. The authors also wish to thank Shmuel Peleg for many helpful suggestions.

1. Introduction

A binary image can be exactly reconstructed if we know the centers and radii of its maximal blocks of 1's, since the set of 1's is the union of these maximal blocks. This representation is called the medial axis transformation (MAT) [1], since the centers of maximal blocks should lie near the midlines of regions of 1's.

Several generalizations of the MAT to grayscale images have been proposed. The binary medial axis (=set of centers of maximal blocks, MA) turns out to be the set of 1's whose distances (=shortest path lengths) to the set of 0's are local maxima [2]. Let us define the gray-weighted distance between two points as the smallest sum of gray levels along any path joining the points; then we can define the gray-weighted medial axis (GRAYMAT) [3] as the set of points whose gray-weighted distances to the set of 0's are local maxima. This definition is not entirely satisfactory, since it gives the set of 0's special status, thus in effect requiring a segmentation of the image; and it is also hard to see how to reconstruct an image from its GRAYMAT.

Another generalization, the SPAN (Spatial Piecewise Approximation by Neighborhoods) [4], finds the largest block, centered at each image point, that satisfies some criterion of homogeneity, and discards blocks if they are contained in other such blocks, thus obtaining a set of maximal blocks. If we know the centers, radii, and mean gray levels of these SPAN blocks, we can

reconstruct a good approximation to the image by superimposing blocks having these gray levels. A disadvantage of this approach is the computational cost of determining the maximal blocks.

A recently proposed generalization, the GRADMAT [5], assigns a score to each image point based on the strengths of the gradient magnitudes (in opposite senses) at pairs of points symmetrically located with respect to the given point. Unfortunately, the GRADMAT turns out to be quite sensitive to noise. In Section 4 we will see that, in consequence, approximations to the image reconstructed from the GRADMAT are rather poor.

A final generalization is based on a characterization of the binary MAT in terms of shrinking and expanding operations [6]. Let S be the set of 1's, let $S^{(k)}$ be the result of repeatedly (k times) "expanding" S by changing all 0's that are adjacent to 1's into 1's, and similarly let $S^{(-k)}$ be the result of k steps of "shrinking" S by changing all 1's that are adjacent to 0's into 0's. It can be shown that $(S^{(-k)})^{(1)} \subseteq S^{(-k+1)}$, and that the difference between these two sets is just the set of MA block centers that have radius k. We can generalize this definition to grayscale images [7] by using local min and max operations as analogs of shrinking and expanding [8]. Let $I^{(k)}$ be the result of k iterations of local max applied to the image I, and let $I^{(-k)}$ similarly be the result of k local mins. It can be shown that $(I^{(-k)})^{(1)} \leq I^{(-k+1)}$. At each image point, we can define a vector $\Delta = (\Delta_1,\ldots,\Delta_m)$ whose kth component is the value

of $I^{(-k+1)}-(I^{(-k)})^{(1)}$ at that point; the array of these vectors constitutes the MMMAT (min-max MAT) of I. Typically, at most points of the image all the components of the MMMAT will have low values, and at most of the exceptional points the values will be high only for a few consecutive values of k, corresponding to the natural "MMMAT radius" at the given point.

The original image $I = I^{(0)}$ can be reconstructed from $I^{(-m)}$ and the MMMAT using a process of iterative local max and addition of Δ values; in fact, $I^{(-k+1)} = (I^{(-k)})^{(1)}+\Delta_k$. However, this exact reconstruction process requires a large amount of information, including the entire array of MMMAT vectors Δ. In Section 2 we will see how good approximations to the image can be constructed using only a few high MMMAT values at a relatively small number of points.

2. MMMAT skeletons

As was seen in [7], summing the components of the MMMAT vector Δ at each point produces a picture P in which the high value points constitute very reasonable skeletons of the original grayscale image I. Since the reconstruction of I involves taking local maxima and adding Δ values, the contribution from points having low values in P will be relatively insignificant. Hence instead of using the entire MMMAT, we can use the Δ vectors only at points where the vector component sum is higher than some threshold. All the other points are treated as if they have zero Δ vectors. Table 1 shows the number of skeleton points in four 64 by 64 images (see Figure 2) when the threshold is set at M/2, M/4 and M/8 where M is the highest value in P, i.e., the highest MMMAT vector sum, for each image. The amount of information used is greatly reduced and the reconstructed image should be a good approximation to the original.

It was also seen in [7] that taking the largest component of the vector Δ at each point also produces good skeletons. This is because, at most points, only a few components of the Δ vector have high values. Thus at each skeleton point we can use only one or a few highest Δ values and still obtain a good reconstructed image.

Thresholding P may produce skeletons that are thick (too many points) or disconnected (too few points). A possible alternative is to apply thinning or line detection operations to P, since the skeleton points should form a set of arcs or curves.

Thinning operations on binary pictures, which repeatedly delete black border points without locally disconnecting their neighborhoods, reduce objects to arcs and curves. This concept has been generalized to grayscale images [9], where each point's gray level is changed to the minimum of its neighbors' gray levels provided this does not locally "disconnect" its neighborhood, where we say that two points are "connected" if there exists a path between them composed of points that are as dark as both of the endpoints.

A simple nonlinear vertical line detection operator assigns to point (i,j) the value $h_v(i,j) = \sum_{k=-1}^{1} [P(i,j+k) - \frac{1}{2}(P(i-1,j+k) + P(i+1,j+k))]$ provided the following six conditions are satisfied:

$P(i,j+k) > P(i-1,j+k)$, $P(i,j+k) > P(i+1,j+k)$ for $k = -1,0,1$.

Operators that detect lines in other directions can be defined analogously [10]. A slightly less strict line detection operator is defined by requiring that five of the six conditions be satisfied. Applying such operators to a skeleton should preserve only the points at local maxima of the cross-sections of the skeleton (i.e., the crests of skeleton "ridges"), thus yielding a thinned skeleton. However, since a point and its neighbors can respond to line detectors in different directions, applying the operators only once to the MMMAT sum can yield lines that are still thick and still contain noise points. If we use an iterative process in which the operator is applied (repeatedly)

to the output of the previous iteration, it should yield skeletons that are quite thin and curve-like.

The thinned skeletons obtained by thinning P or applying line detectors to P can be used for reconstruction. Table 2 shows the numbers of points in the skeletons obtained using these methods. Figure 1 shows the skeletons of the chromosome image (see Figure 2) using the thresholding, thinning, and line detecting techniques. The six-condition line detector was iterated twice and the five-condition line detector was iterated three times. The line detection results yield skeletons that are quite thin and curve-like.

3. Reconstruction from the MMMAT

Four images were used in the experiment. The MMMAT's were obtained using eight-neighbor local min and local max operations. Figure 2 shows the original images and the reconstructed images using the points whose MMMAT vector sums $\sum_{i=1}^{m} \Delta_i$ are greater than M/4 where M is the maximum MMMAT sum in the image. As we can see from Table 1, the numbers of points used are quite small, but the results are very good.

In the tank image, the background near the top image border has a few dark areas. Thus the MMMAT sums at a few of the points there have values between M/2 and M/4. In the reconstructed image where M/4 was used as a threshold to select skeleton points, the nonhomogeneity of the background is exaggerated (see Figures 2,3). If the threshold is set at M/2 then these background blocks disappear (see Figure 4).

Figure 3 shows reconstructions using the same skeleton points as in Figure 2, but using only a few (1, 2, or 3) highest Δ values at each point. Using three Δ values is almost the same as using the entire Δ vector. Good approximations to the images can be obtained using only a single Δ value at each of these points.

Figure 4 shows that the points with MMMAT sums > M/2 are not sufficient to reconstruct a good approximation to the original image. The M/4 skeleton with one Δ value gives better approximations than the M/2 skeleton with five Δ values. The M/8

skeletons have 60% to 100% more points than the M/4 skeletons, but the reconstructed images are at best slightly improved.

Figures 5, 6, and 7 are reconstructions using the skeleton points obtained from thinning and line detection. These skeletons are more curve-like, but thresholding with M/4 seems to give better approximations to the original images.

To see how noise in the images affects reconstruction from the MMMAT, we added noise (mean = 0, standard deviation = 5) to the chromosome picture, and then performed the reconstruction process. The original and the reconstructed images using different skeleton point selection methods are shown in Figure 8. Thresholding with M/4 works better than thinning and line detection even though it uses fewer points. Thresholding with M/4 and using three Δ values at each selected point reconstructs a reasonable approximation to the chromosome picture with most of the noise removed.

Figure 9 shows the skeletons of the image obtained by applying thresholding, thinning and line detection to the MMMAT sum picture. As can be seen from Figure 9(a), there are too few points with MMMAT sum ($\Sigma\Delta_i$) > M/2, where M is the highest MMMAT vector sum for the image; and there are many isolated points with $M/2 \geq \Sigma\Delta_i > M/4$ (compare Figures 1a and 9a). The skeletons obtained from thinning and line detection contain curve segments that are not in the "centers" of the objects; rather, they arise from points whose $\Sigma\Delta_i$ values are quite low,

i.e. $\leq$ M/4 (see the points labelled "8" in Figure 9a). If we modify our skeleton point selection procedure by applying the line detector or the thinning operator to the MMMAT sum picture semithresholded at M/4 (i.e., points with values $\leq$ M/4 are set to zero), we obtain quite reasonable skeletons such that most of the isolated points with $\Sigma\Delta_i$ > M/4 are no longer part of the skeleton; see Figure 10. This is particularly noticeable in the line detection case. The numbers of points in these skeletons are only 42 and 177 (see Table 3). Figure 11 shows that reconstructions from these small numbers of points give fair approximations to the original chromosome image, with much of the noise removed.

4. Reconstruction from the GRADMAT

The GRADMAT skeleton is quite sensitive to the presence of noise edges or irregularities in the region edges. In this section we discuss possible ways to reconstruct an image from the high score points of its GRADMAT.

Each image point p's GRADMAT value is a score based on the gradient magnitudes at pairs of points that have p as their midpoint. If each point p stores the coordinates and gradient magnitudes of all the pairs of points q making contributions to its score, then one way to reconstruct an approximation to the image is to "color" all the points between each pair of q's with the corresponding gradient magnitude. In case a point receives more than one gradient value, the maximum is used. However, the amount of information needed at each point in order to do this is too large.

Alternatively, instead of trying to use all pairs of contributing points, we can choose a radius r which provides the strongest response and color all the points in the disk of radius r with the score of p. However, this would certainly produce objects that are too big, as too many points are colored in. A modification is to color only a rectangular strip having p at its center and length 2r where its width and orientation are determined by the responses from the points on the circle C of radius r centered at p, i.e., all the points at distance r from p, as follows: Divide C into sixteen equal length arcs. For each

pair of opposite arcs, calculate the total score contribution from the points on them. Let X be the sector angle corresponding to the longest consecutive sequence of arcs with nonzero contributions. The major axis of the rectangle is located in the direction of X/2. Various widths have been tried in the reconstruction. Figure 12(b) shows the reconstruction using width $2r \sin(X/4)$. The objects are somewhat too big, and have irregular boundaries. Figure 12(c) shows the reconstruction using width $2r \sin(X/8)$; the objects are smaller, but even more irregular. Figure 12(d) is the reconstructed image using rectangles of length r and width 1, i.e., a line joining the two opposite edge points on C which give the maximal contribution to the score of p. The objects are now too small and quite ragged. Thus we see that reconstruction from the GRADMAT produces objects whose general shapes are good approximations of the original objects, but the results are not as good as those using the MMMAT.

5. Concluding remarks

Using a small amount of information, namely, a set of points having high MMMAT values and a few components that make strong contributions to these values, good approximations to grayscale images can be reconstructed. Hence these points with their appropriate Δ values form a compact representation of the image. Both the MMMAT skeleton and the reconstruction computation are relatively inexpensive and computable in parallel. The examples show that they give better approximations than reconstructions from the SPAN [4] or GRADMAT.

The MAT is not just a compact representation of a binary image; it also provides important structural and shape information. The MAT points tend to lie on a set of arcs corresponding to "lobes" of the set S, and the way the radius varies along such an arc provides information about its shape (width, taper, etc.). Analogously, it should be possible to extract certain types of "shape" information from an unsegmented gray level image by inspecting its generalized MAT.

References

1. H. Blum, A transformation for extracting new descriptors of shape, in W. Wathen-Dunn, ed., Models for the Perception of Speech and Visual Form, MIT Press, Cambridge, MA, 1967, 362-380.

2. A. Rosenfeld and J. L. Pfaltz, Sequential operations in digital picture processing, J.ACM 13, 1966, 471-494.

3. G. Levi and U. Montanari, A grey-weighted skeleton, Info. Control 17, 1970, 62-91.

4. N. Ahuja, L. S. Davis, D. L. Milgram, and A. Rosenfeld, Piecewise approximation of pictures using maximal neighborhoods, IEEETC-27, 1978, 375-379.

5. S. Wang, A. Rosenfeld, and A. Y. Wu, A medial axis transformation for grayscale pictures, TR-843, Computer Vision Laboratory, Computer Science Center, University of Maryland, College Park, MD, December 1979.

6. J. C. Mott-Smith, Medial axis transformations, in B. S. Lipkin and A. Rosenfeld, eds., Picture Processing and Psychopictorics, Academic Press, NY, 1970, 267-278.

7. S. Peleg and A. Rosenfeld, A min-max medial axis transformation, TR-856, Computer Vision Laboratory, Computer Science Center, University of Maryland, College Park, MD, January 1980.

8. Y. Nakagawa and A. Rosenfeld, A note on the use of local min and max operations in digital picture processing, IEEETSMC-8, 1978, 632-635.

9. C. R. Dyer and A. Rosenfeld, Thinning algorithms for gray-scale pictures, IEEETPAMI-1, 1979, 88-89.

10. A. Rosenfeld and A. C. Kak, Digital Picture Processing, Academic Press, NY, 1976, 310-314.

	M/2	M/4	M/8
Chromosomes	74	189	322
Terrain	244	582	1268
Tank	30	227	552
Blood Cell	74	462	721

Table 1. Number of skeleton points in four 64x64 images (see Figure 2) using various thresholds (M = highest MMMAT sum in image).

		Line detection	
	Thinning	Six conditions	Five conditions
Chromosomes	166	127	208
Terrain	486	324	557
Tank	276	196	264
Blood Cell	277	321	457

Table 2. Number of skeleton points in the four images after thinning or line detection.

Thresholding at M/4	257
Thinning	275
Line detection	300
Thinning after semithresholding at M/4	177
Line detection after semithresholding at M/4	42

Table 3. Numbers of skeleton points obtained from the chromosome image of Figure 7a using various selection techniques.

Figure 1. Skeletons of chromosome image (see Figure 2) obtained using various techniques.

(a) Thresholding. 2 indicates points with value > M/2
4 indicates points with M/2 ≥ value > M/4
8 indicates points with M/4 ≥ valie > M/8

(b) Thinning.

(c) Line detection (6 conditions).

(d) Line detection (5 conditions).

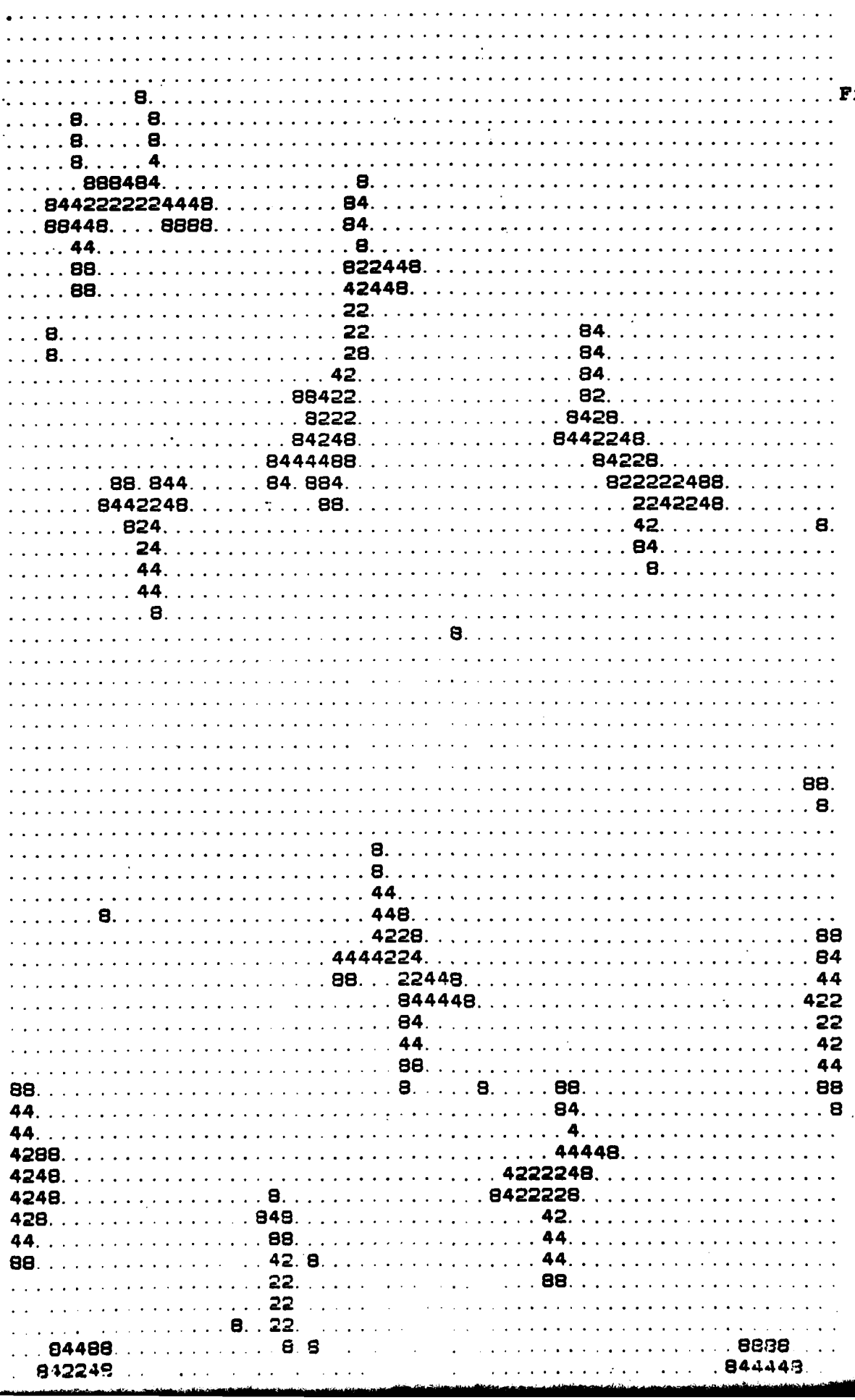

Figure 1a.

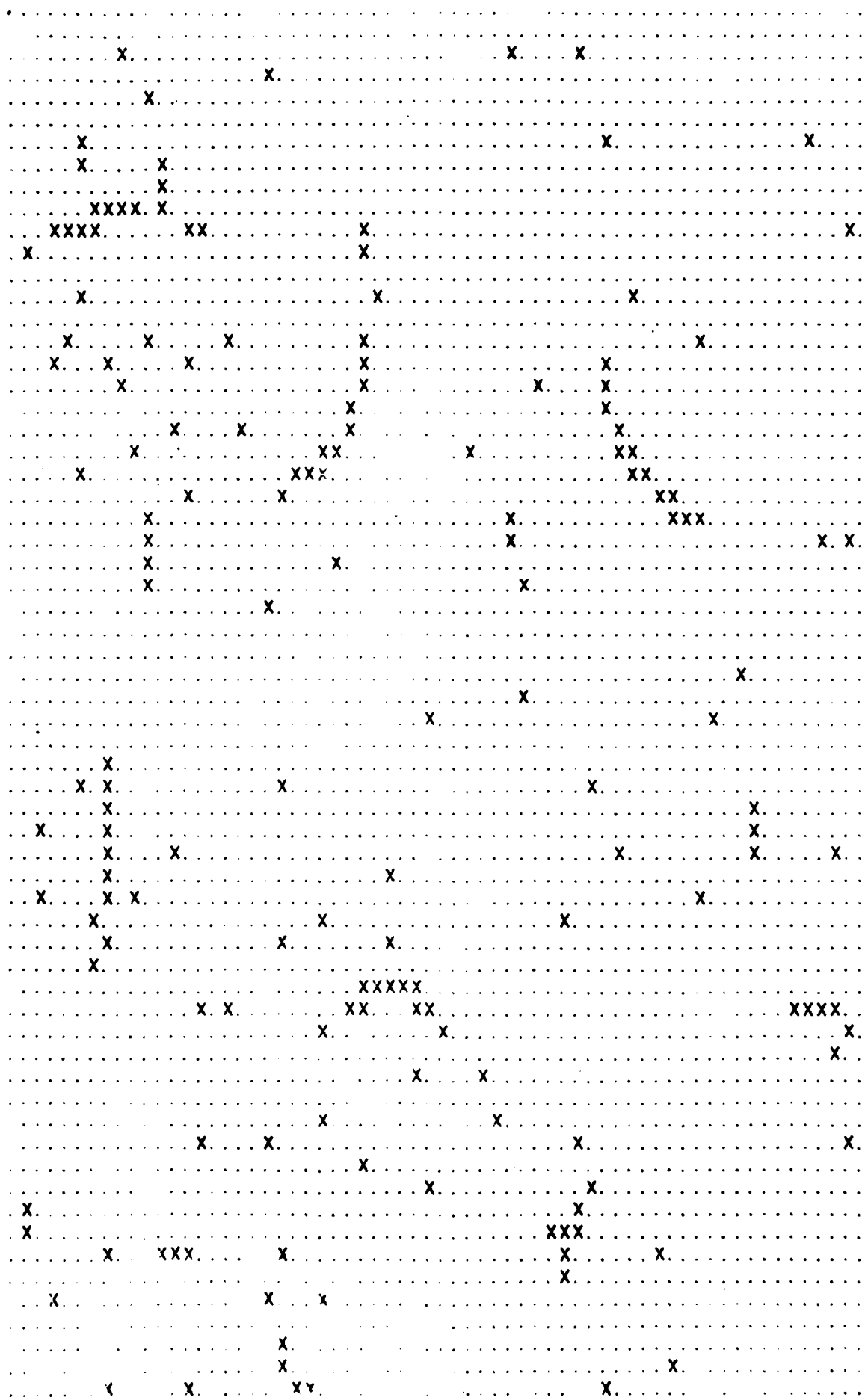

Figure 1b.

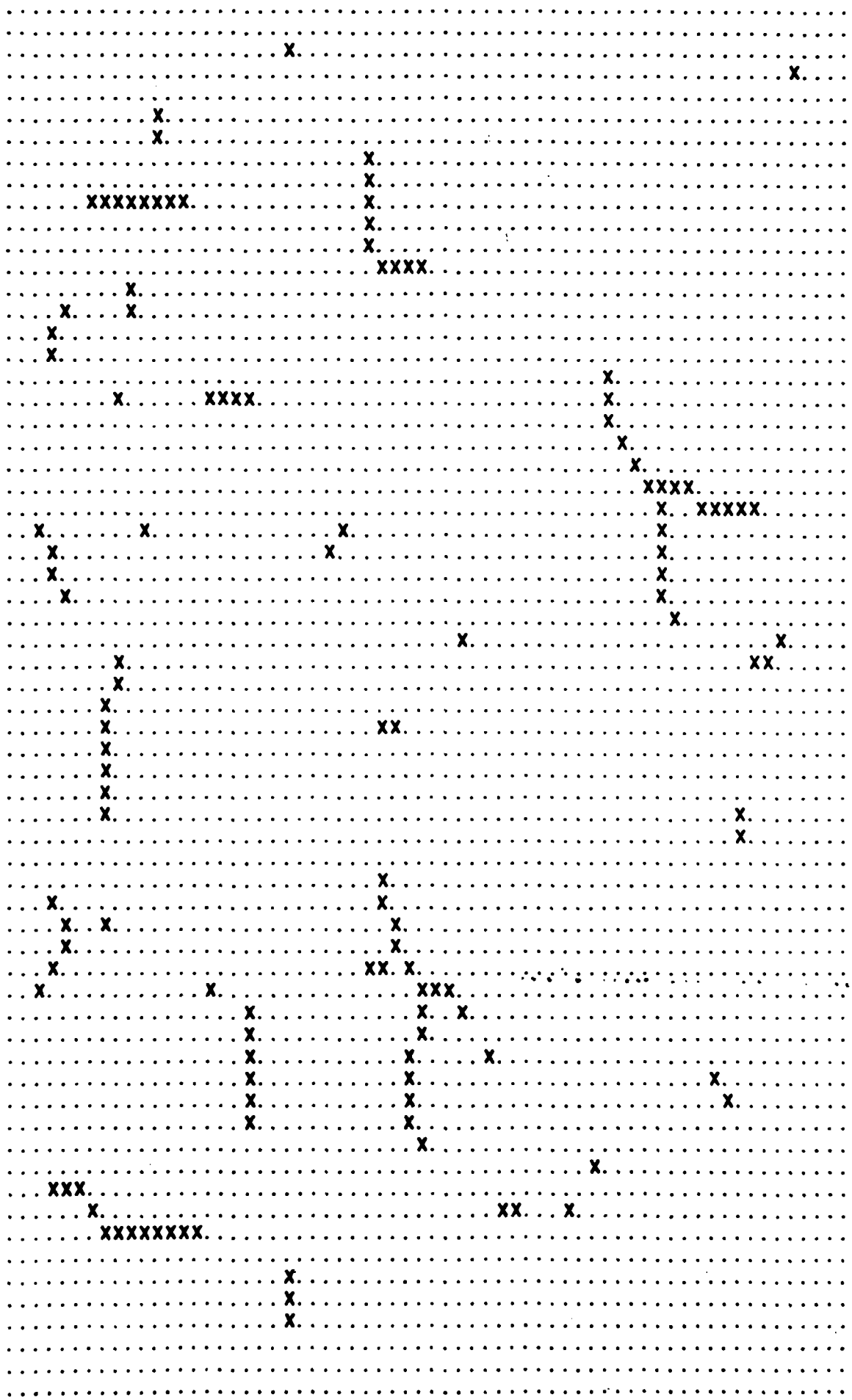

Figure 1c.

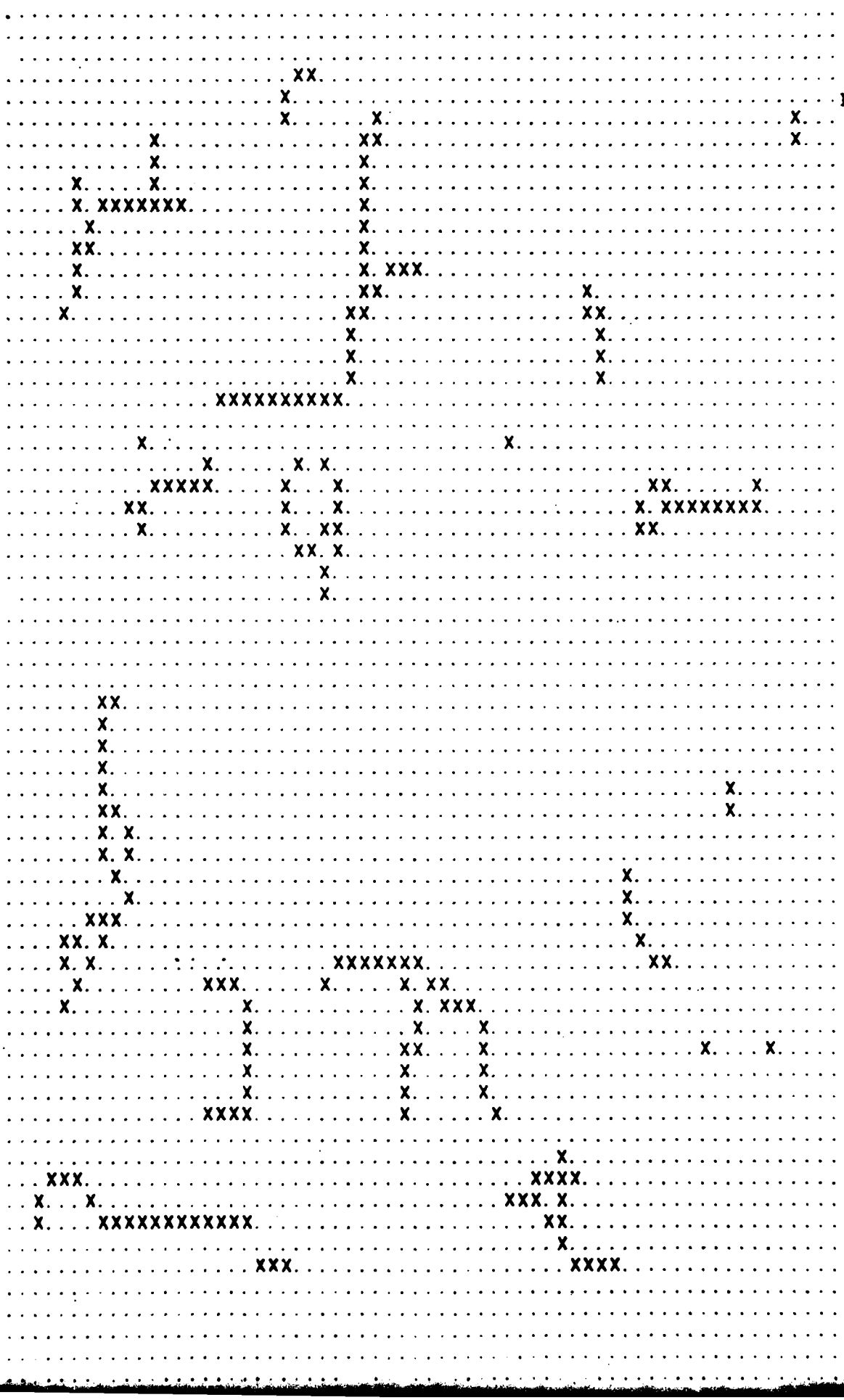

Figure 1d.

(i)

(ii)

(iii)

(iv)

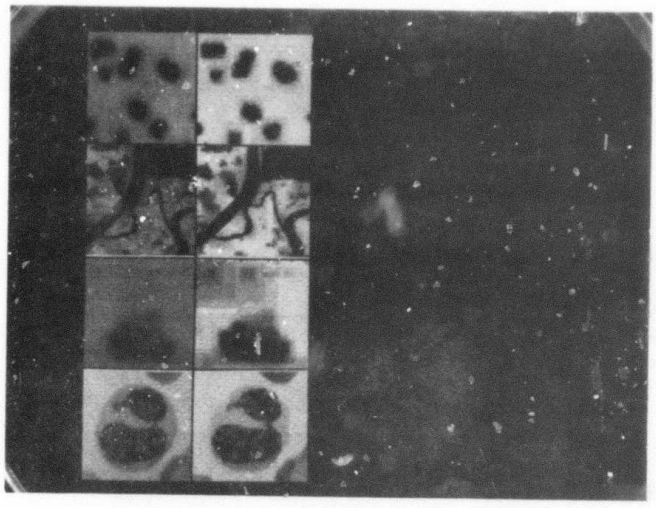

(a) (b)

Figure 2. Reconstruction from the MMMAT using points whose MMMAT vector sums are greater than M/4. (a) Original images; (b) reconstructed images; (i) chromosomes; (ii) terrain; (iii) tank; (iv) blood cell.

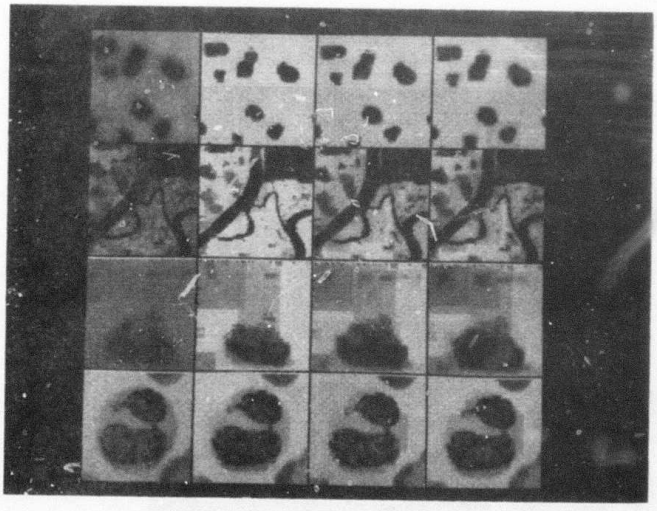

(a) (b) (c) (d)

Figure 3. Same as Figure 2 except
Column (a): Original image
Column (b): Reconstruction using the maximum Δ value at each point having sum > M/4
Column (c): Reconstruction using the two largest Δ values at each such point
Column (d): Reconstruction using the three largest Δ values at each such point

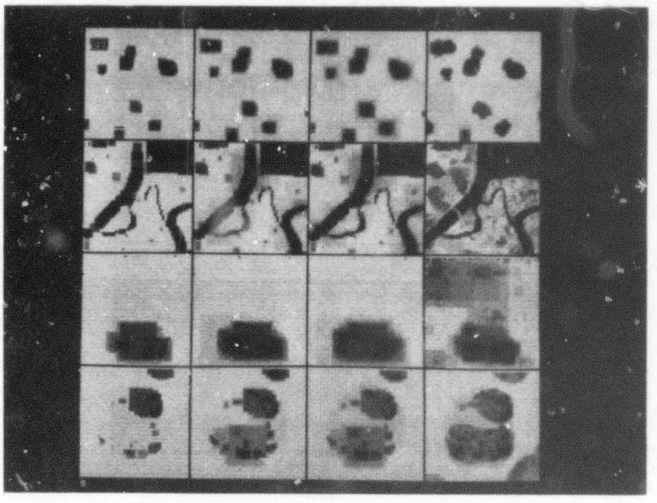

(a) (b) (c) (d)

Figure 4.
(a) Reconstructed images using the largest Δ value at points whose MMMAT vector sums are greater than M/2.
(b) Same as (a) except that the three largest Δ values at each point are used
(c) Same as (a) except that the five largest Δ values at each point are used
(d) Same as (a) except that all points with MMMAT vector sums greater than M/8 are used.

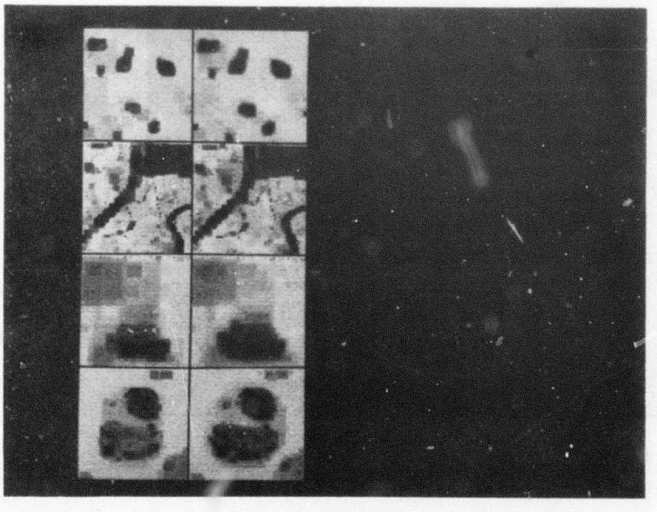

(a) (b)

Figure 5. Reconstruction using points obtained by thinning the MMMAT sums.
(a) The largest Δ values are used
(b) The three largest Δ values are used

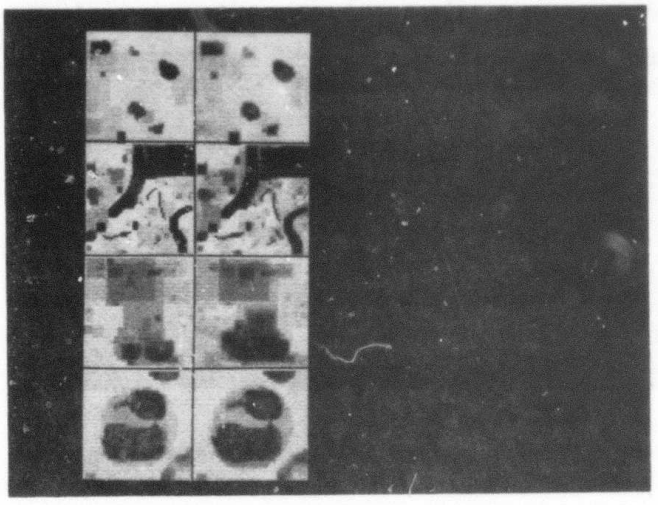

(a) (b)

Figure 6. Same as Figure 5 except that points satisfying a nonlinear line detector (six conditions) are used.

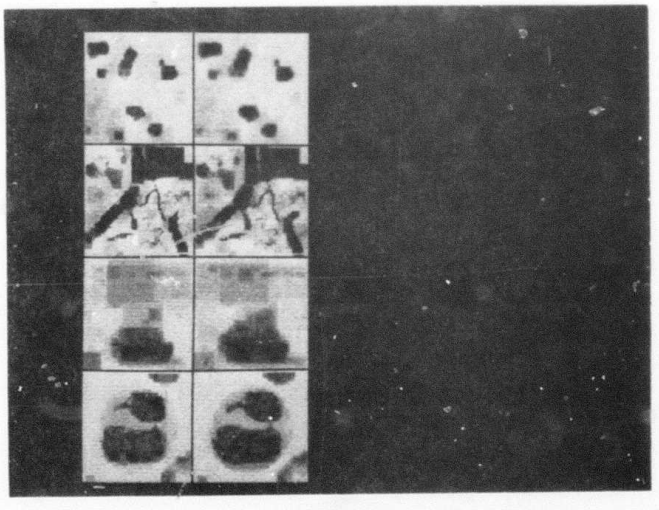

(a) (b)

Figure 7. Same as Figure 5 except that points satisfying a less strict nonlinear line detector (five conditions) are used.

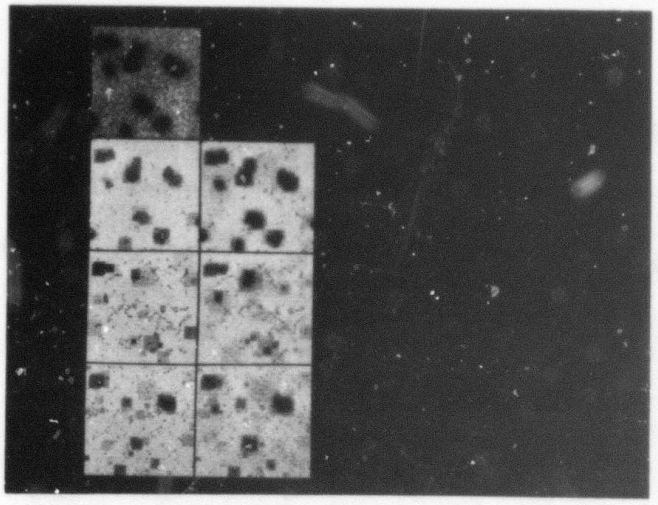

Figure 8. Reconstruction of a noisy chromosome image
(a) Chromosomes of Figure 2(a) with noise added (mean = 0, standard deviation = 5 on a grayscale of 0-63)
(b) Reconstruction of (i) using points with MMMAT sum > M/4 and the largest Δ value at each of these points
(c) Same as (b) escept that the three largest Δ values are used
(d),(e) Same as (b),(c) except that points obtained from the nonlinear line detector are used
(f),(g) Same as (b),(c) except that points obtained from thinning are used.

Figure 9. Skeletons of the noisy chromosome image (Figure 7a) using various techniques.

(a) Thresholding. 2 indicates points with value > M/2
4 indicates points with M/2 ≥ value > M/4
8 indicates points with M/4 ≥ value > M/8
(b) Thinning.
(c) Nonlinear line detection.

Figure 10. Skeletons of the noisy chromosome image obtained by applying
(a) Thinning operator
(b) Nonlinear line detector
to the MMMAT sum picture semithresholded at M/4.

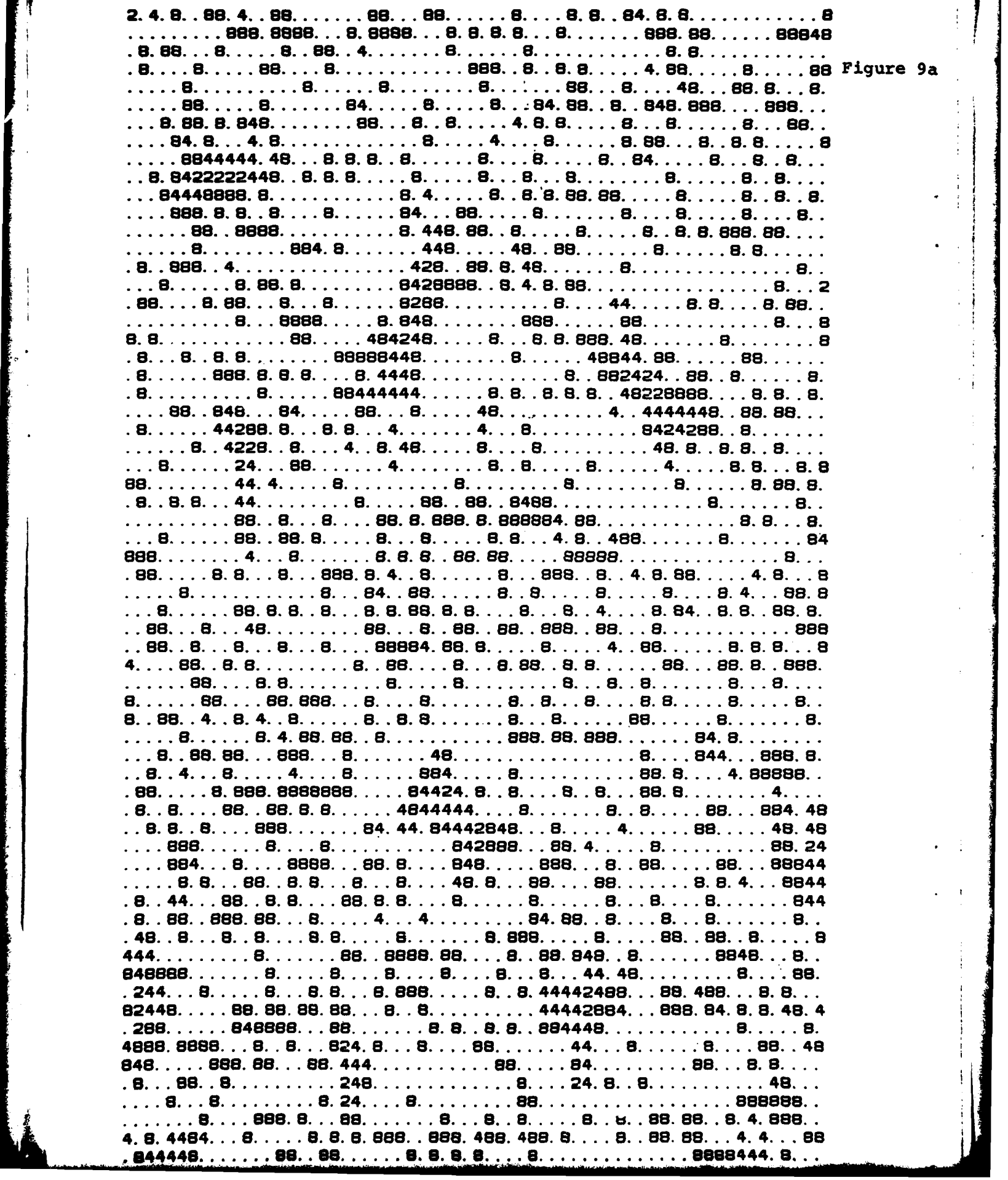

Figure 9a

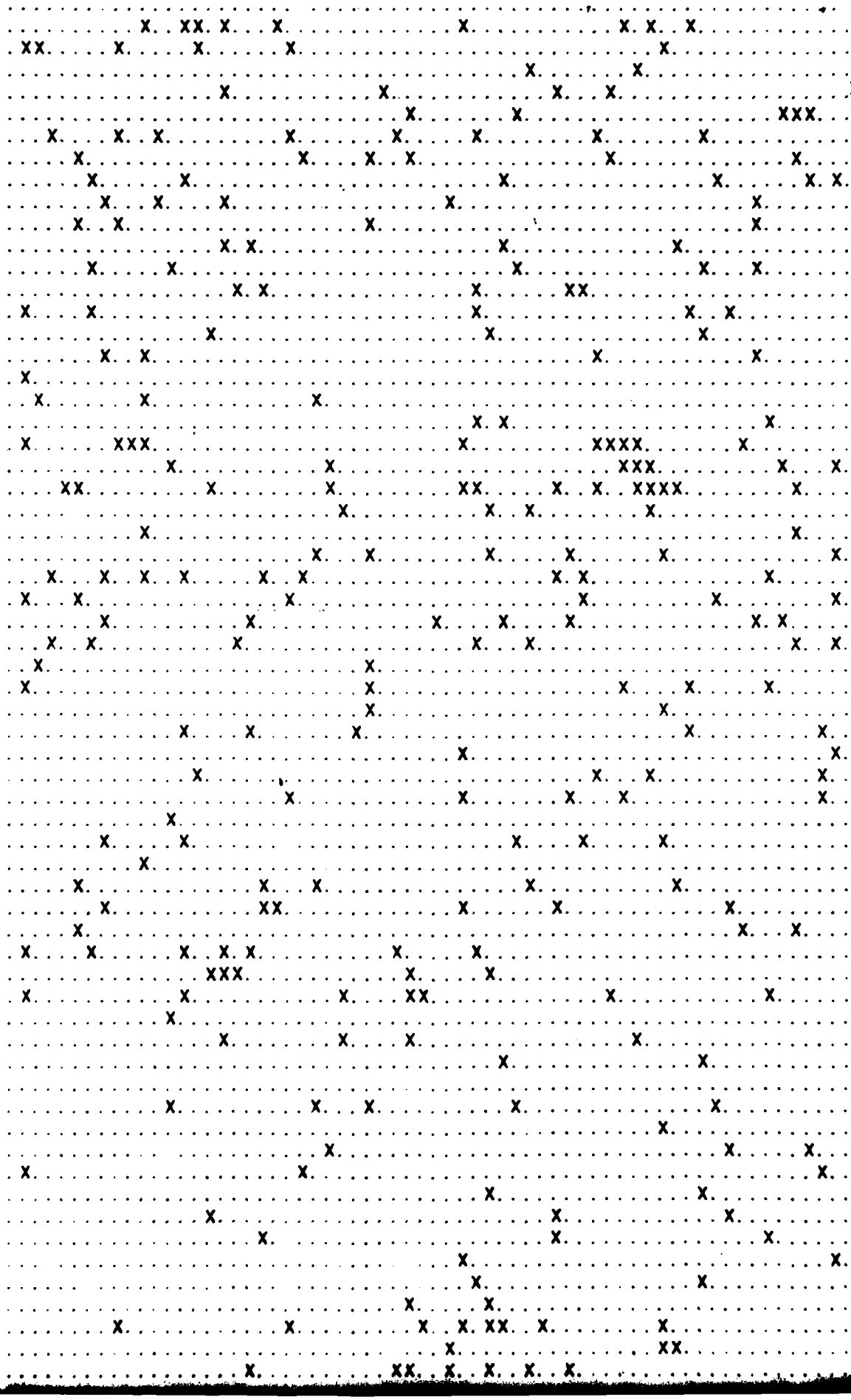

Figure 9b

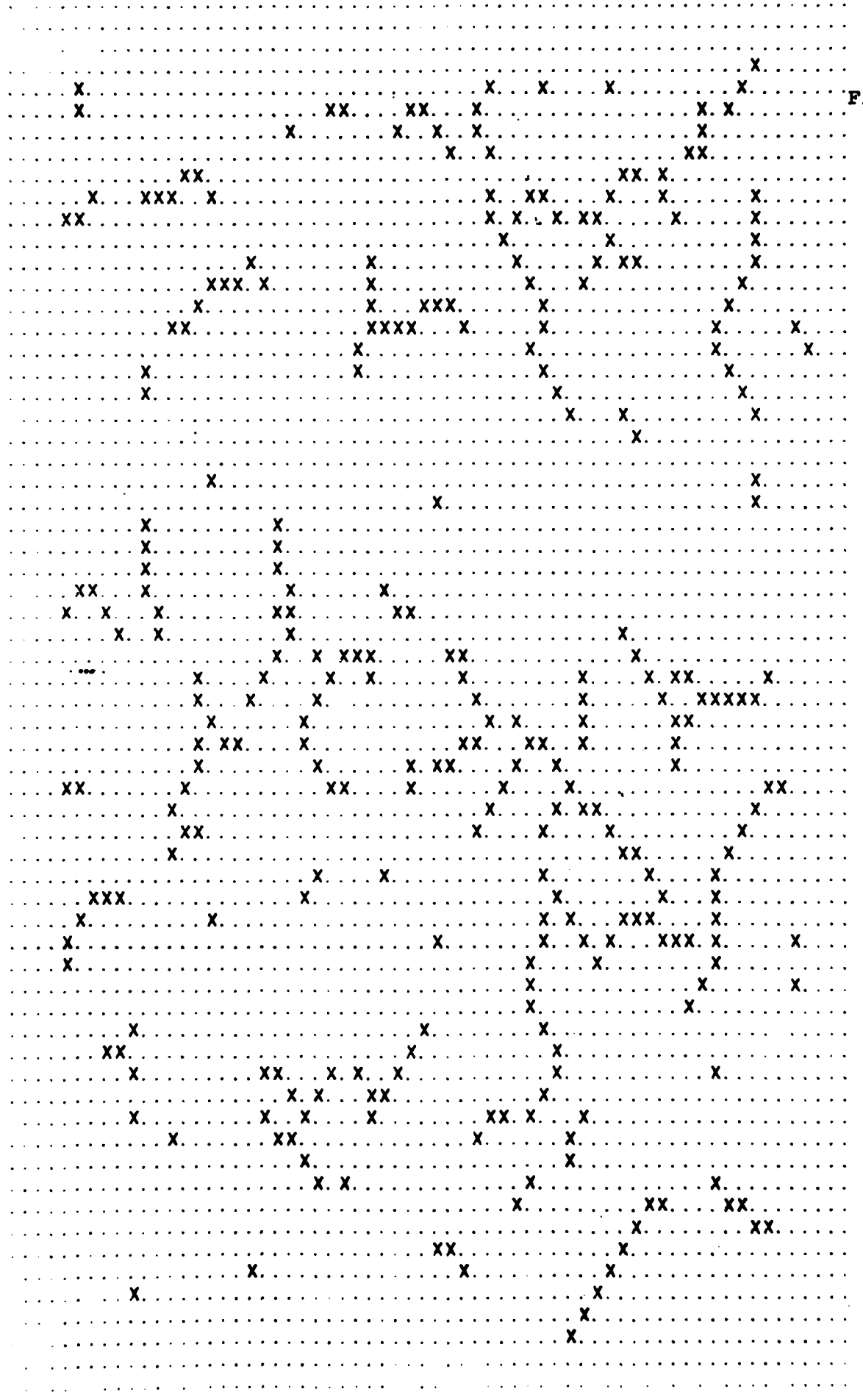

Figure 9c

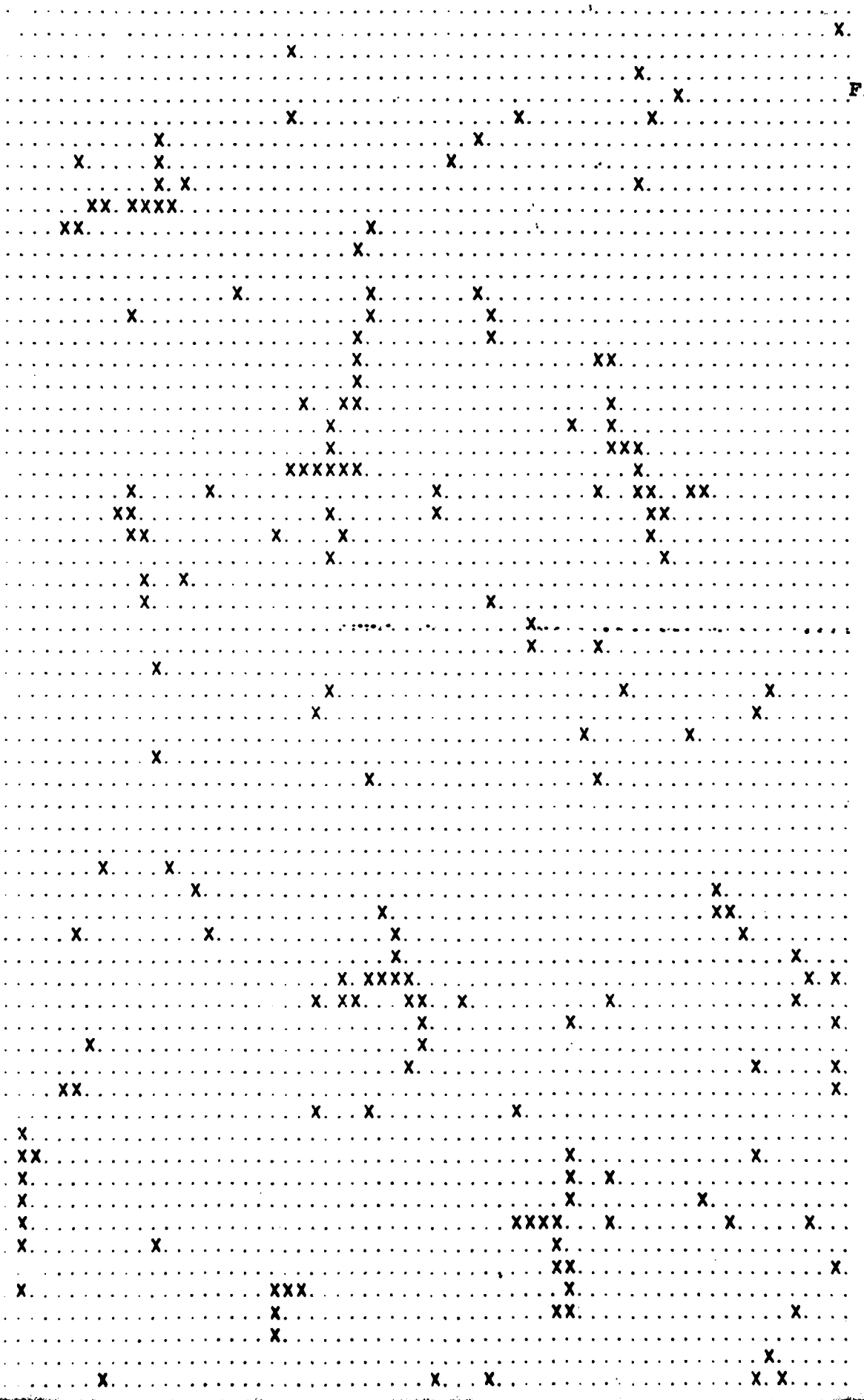

Figure 10a

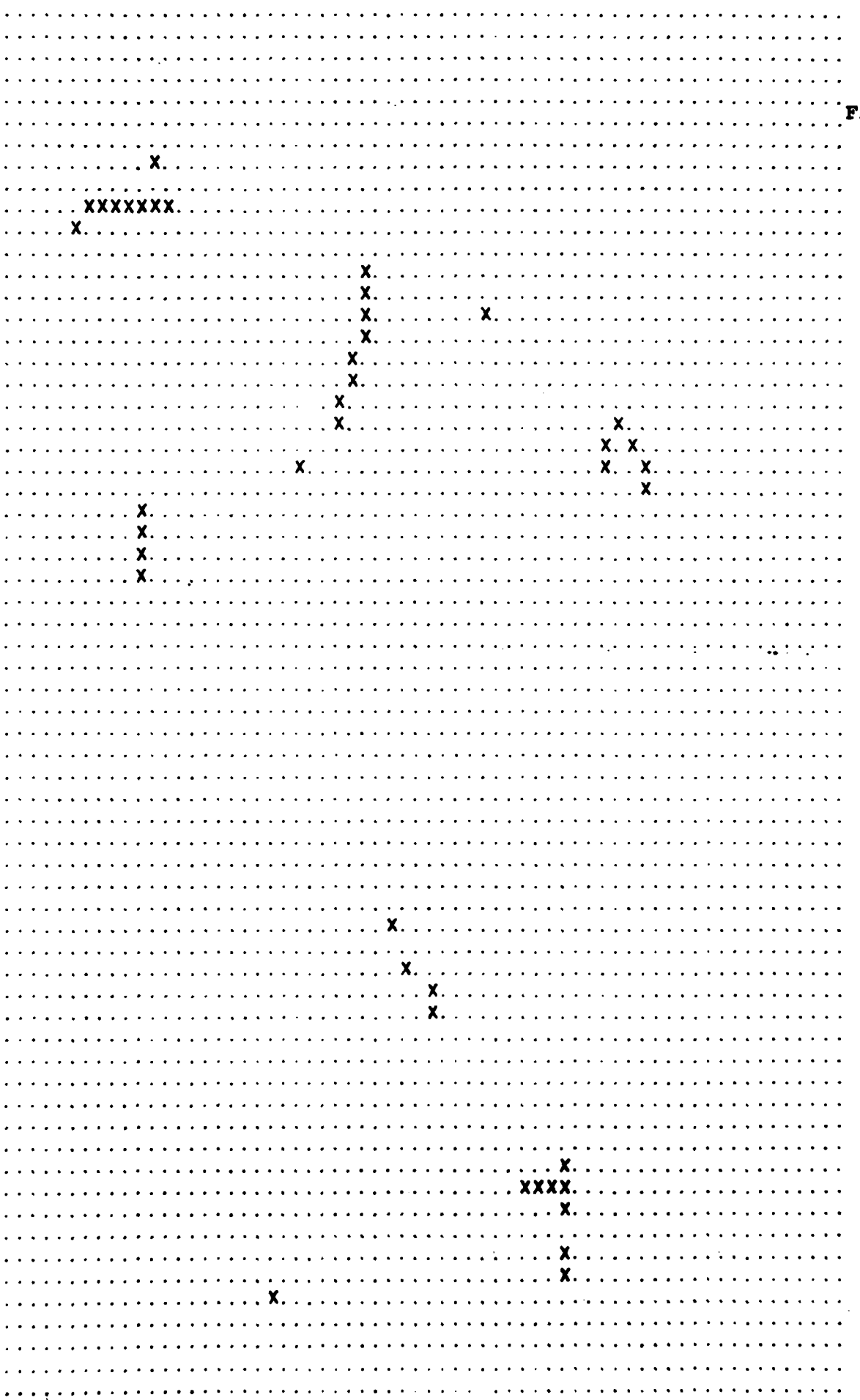

Figure 10b

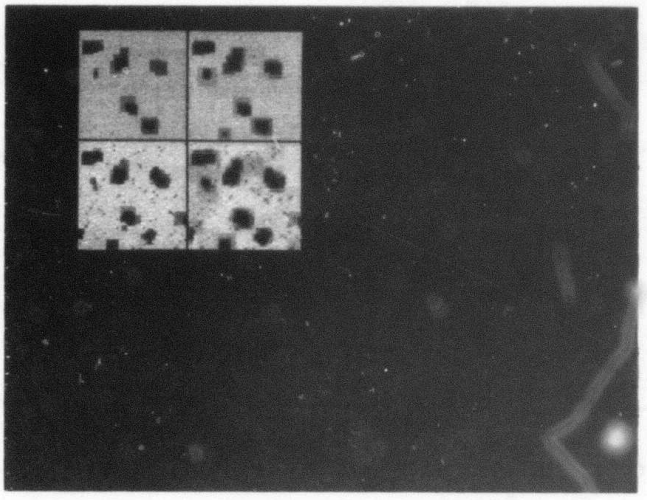

Figure 11. Reconstruction of the noisy chromosome image of Figure 8(a).
(a) Using skeleton points obtained by applying the nonlinear line detector to the MMMAT sum picture semithresholded at M/4, and the largest Δ value at each of these points
(b) Same as (a) except that the three largest Δ values are used
(c),(d) Same as (a),(b) except that the thinning operator is used

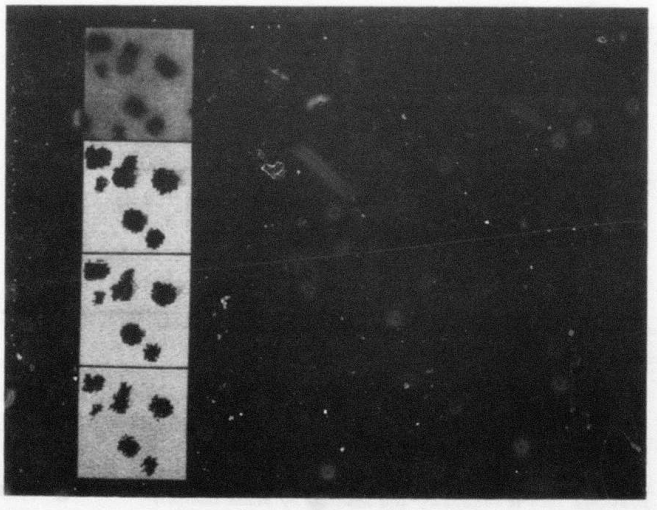

Figure 12. Reconstructions from the GRADMAT
(a) Original image
(b) Reconstruction using rectangles
(c) Reconstruction using rectangles as in (b) but with sector angle reduced by a factor of 2
(d) Reconstruction using lines

UNCLASSIFIED

SECURITY CLASSIFICATION OF THIS PAGE (When Data Entered)

REPORT DOCUMENTATION PAGE

READ INSTRUCTIONS BEFORE COMPLETING FORM

1. REPORT NUMBER

2. GOVT ACCESSION NO. AD-A092 993

3. RECIPIENT'S CATALOG NUMBER

4. TITLE (and Subtitle)

(6) IMAGE APPROXIMATION FROM GRAYSCALE "MEDIAL AXES".

5. TYPE OF REPORT & PERIOD COVERED

(9) Technical rept.,

6. PERFORMING ORG. REPORT NUMBER

(14) TR-900

7. AUTHOR(s)

(10) Shyuan Wang
Angela Y. Wu
Azriel Rosenfeld

(12) 33

8. CONTRACT OR GRANT NUMBER(s)

DAAG-53-76C-0138

9. PERFORMING ORGANIZATION NAME AND ADDRESS

Computer Vision Laboratory, Computer Science Center, University of Maryland, College Park, MD 20742

10. PROGRAM ELEMENT, PROJECT, TASK AREA & WORK UNIT NUMBERS

(11) May 80

11. CONTROLLING OFFICE NAME AND ADDRESS

U.S. Army Night Vision Laboratory
Ft. Belvoir, VA 22060

12. REPORT DATE

May, 1980

13. NUMBER OF PAGES

32

14. MONITORING AGENCY NAME & ADDRESS (if different from Controlling Office)

(15) DAAG53-76-C-0138
DARPA Order-3206

15. SECURITY CLASS. (of this report)

Unclassified

15a. DECLASSIFICATION/DOWNGRADING SCHEDULE

16. DISTRIBUTION STATEMENT (of this Report)

Approved for public release; distribution unlimited.

17. DISTRIBUTION STATEMENT (of the abstract entered in Block 20, if different from Report)

18. SUPPLEMENTARY NOTES

19. KEY WORDS (Continue on reverse side if necessary and identify by block number)

Image processing
Pattern recognition
Image approximation
Medial axis transformations

20. ABSTRACT (Continue on reverse side if necessary and identify by block number)

Several types of gray-weighted "medial axes" have been defined. This paper shows that one of them, the min-max medial axis, can be used to reconstruct good approximations to the original image based on a relatively small amount of information.

DD FORM 1 JAN 73 1473 EDITION OF 1 NOV 65 IS OBSOLETE

UNCLASSIFIED

SECURITY CLASSIFICATION OF THIS PAGE (When Data Entered)